Supporting Information

Crosslinked, highly-conductive binder unlocks low-temperature silicon anodes for lithium-ion batteries

Yihong Yao,[a,§] Yaozong Yang,[a,§] Zhijie Jiang,[c,*] Zhaolin Li,[a] Sihong Du,[c] Jie Wang,[a,b] Ying Luo,[d] Jingying Xie,[d] and Hailei Zhao[a,b,*]

[a] School of Material Science and Engineering, University of Science and Technology Beijing, Beijing 100083, China

[b] Beijing Municipal Key Laboratory of New Energy Materials and Technologies, Beijing 100083, China

[c] Beijing Xiaomi Mobile Software Co., Ltd. Beijing 100085, China

[d] State Key Laboratory of Space Power-Sources Technology, Shanghai Institute of Space Power-Sources, Shanghai 200245, China

[§] These authors contributed equally to this work.

* Corresponding author at: School of Materials Science and Engineering, University of Science and Technology Beijing, Beijing 100083, China.

E-mail address: hlzhao@ustb.edu.cn (H. Zhao).

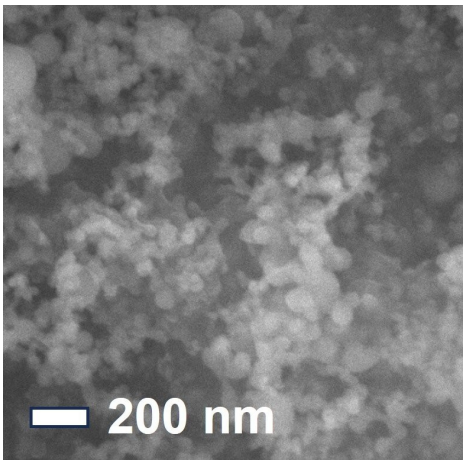

Figure S1. SEM image of Si power.

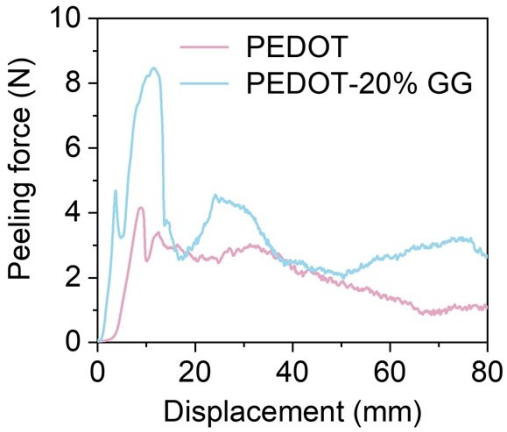

Figure S2. 180° peeling tests of PEDOT@Si and PEDOT-20%GG@Si electrodes on Cu foil current collectors.

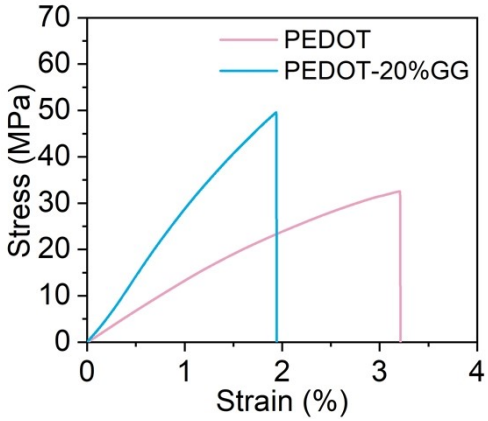

Figure S3. Tensile stress-strain curves of studied two binder films PEDOT and PEDOT-20%GG.

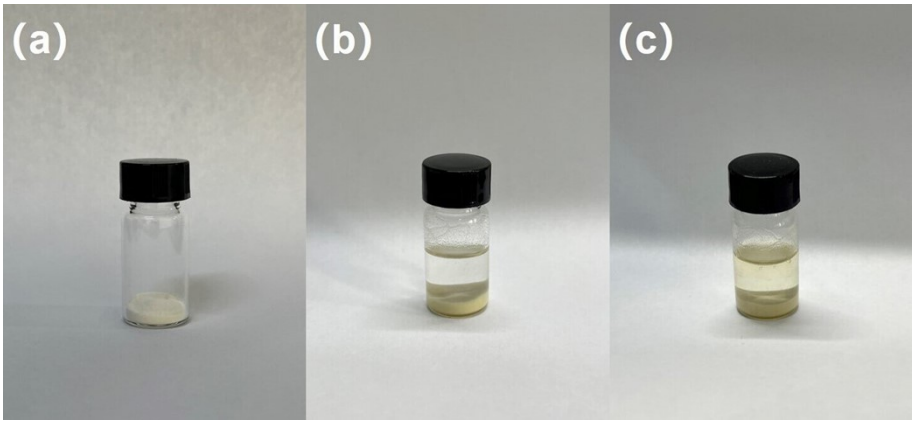

Figure S4. Photoes of GG (a) and mixture of GG and electrolyte after 0 (b) and 24 h (c).

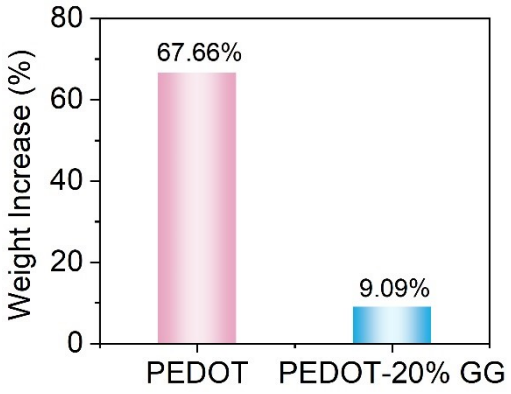

Figure S5. Swelling performance test of binders PEDOT and PEDOT-20%GG.

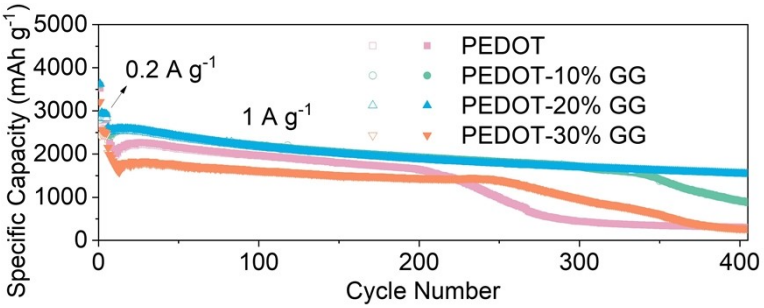

Figure S6. Cycling performance of PEDOT@Si, PEDOT-10%GG@Si, PEDOT-20%GG@Si, and PEDOT-30%GG@Si electrodes at a current density of 1 A g^{-1}.

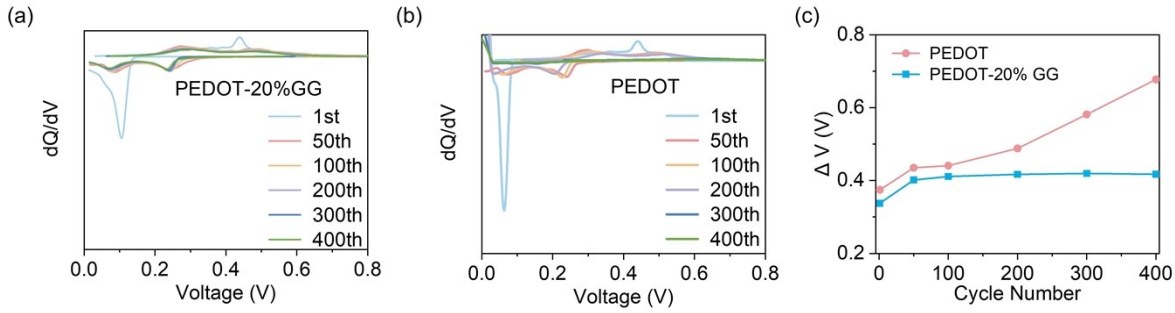

Figure S7. Plots of dQ/dV vs. voltage of electrodes PEDOT-20%GG@Si (a) and PEDOT@Si (b) at different cycles. (c) Voltage difference of electrodes PEDOT-20%GG@Si and PEDOT@Si.

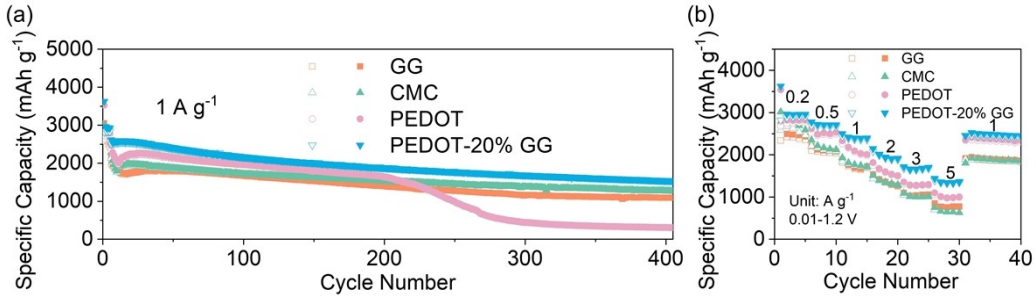

Figure S8. (a) Cycling performance of electrodes GG@Si, CMC@Si, PEDOT@Si, PEDOT- and 20%GG@Si at a current density of 1 A g^{-1}. (b) Rate performance of electrodes GG@Si, CMC@Si, PEDOT@Si, and PEDOT-20%GG@Si.

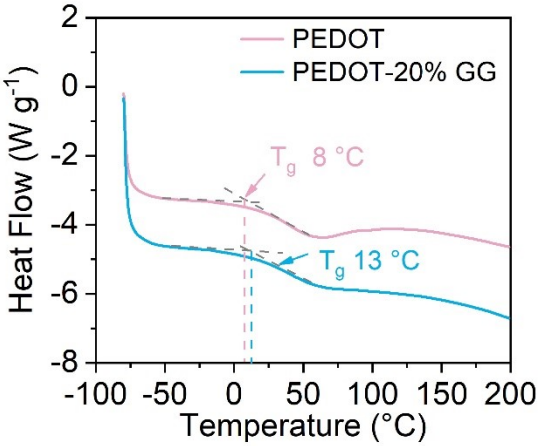

Figure S9. DSC curves of two binder films PEDOT and PEDOT-20%GG.

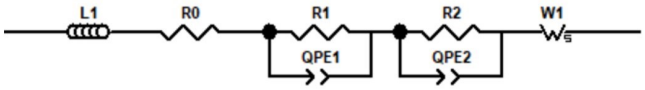

Figure S10. Equivalent circuit of Nyquist plot.

Table S1. Fitting parameters of EIS results of Si electrode with different binders at different cycles based on the data in Figure 5.

Sample	Cycle number	R_0 (Ω)	R_f (Ω)	R_{ct} (Ω)
PEDOT	20	2.753	5.083	34.83
	400	7.645	11.46	45.07
PEDOT-20%GG	20	3.302	5.065	12.01
	400	5.987	6.181	28.77

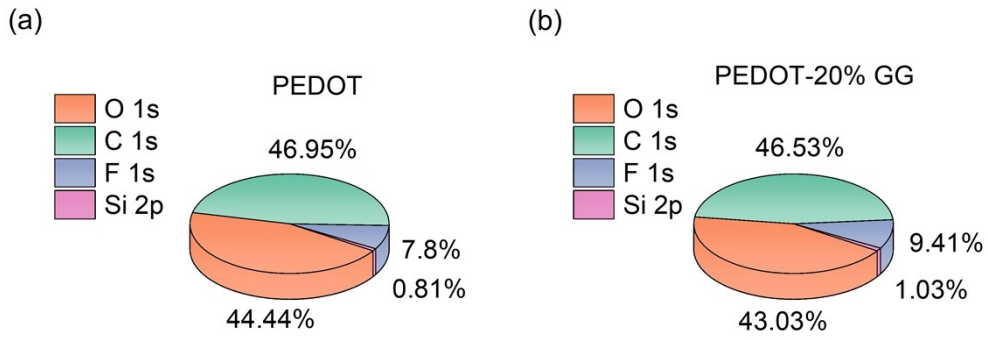

Figure S11. Diagram of content of each element in the SEI film of electrodes PEDOT@Si (a) and PEDOT-20%GG@Si (b) respectively, after 50 cycles, according to XPS results.

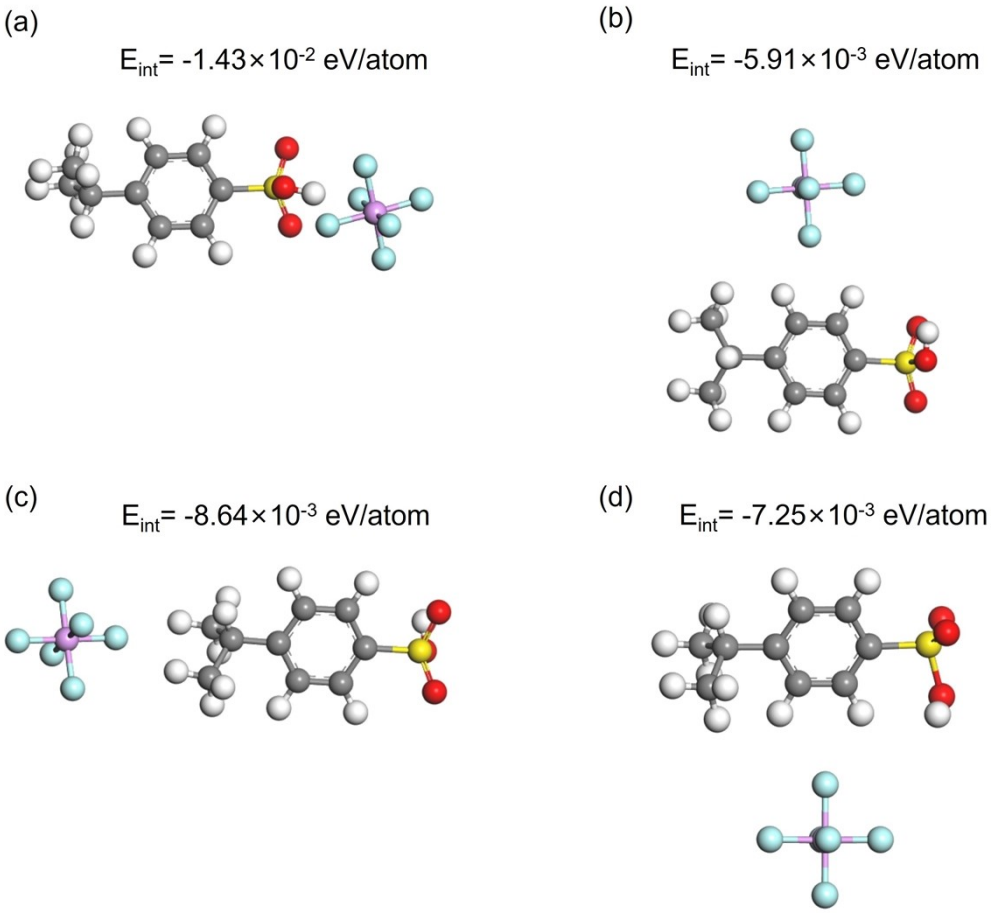

Figure S12. Calculation molecular structure and the obtained binding energy between PSS and PF_6^-.

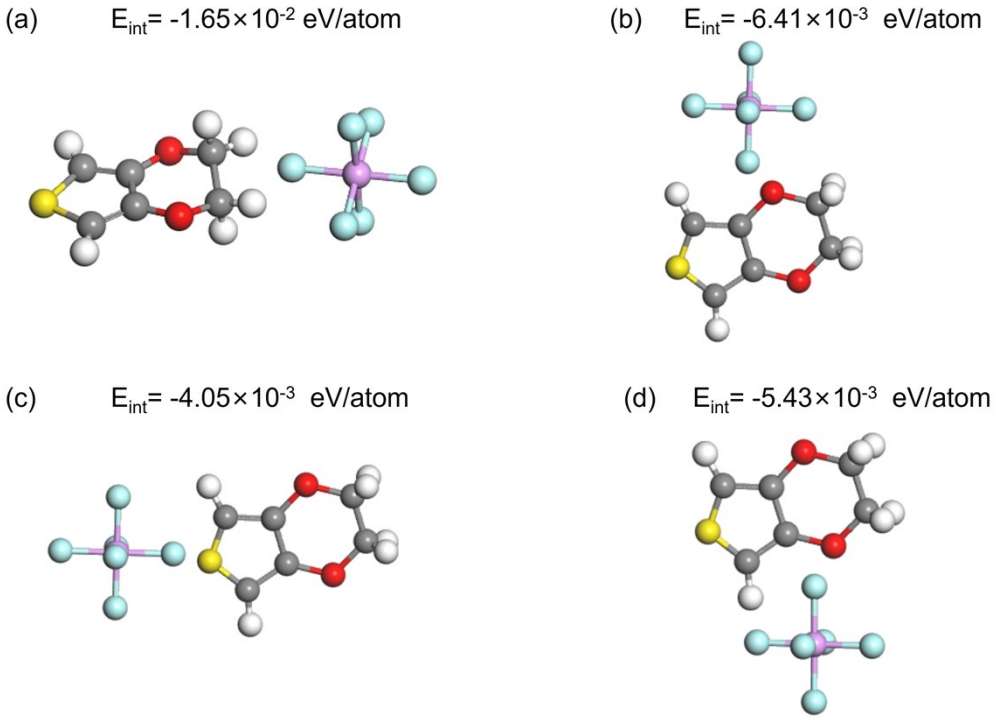

Figure S13. Calculation molecular structure and the obtained binding energy between PEDOT and PF_6^-.